LETTERS

A ground-layer adaptive optics system with multiple laser guide stars

M. Hart[1], N. M. Milton[1], C. Baranec[2], K. Powell[1], T. Stalcup[3], D. McCarthy[1], C. Kulesa[1] & E. Bendek[1]

To determine the influence of the environment on star formation, we need to study the process in the extreme conditions of massive young star clusters (~10^4 solar masses) near the centre of our own Galaxy[1,2]. Observations must be carried out in the near infrared because of very high extinction in visible light within the Galactic plane. We need high resolution to identify cluster members from their peculiar motions[3], and because most such clusters span more than 1′, efficient observation demands a wide field of view. There is at present no space-based facility that meets all these criteria. Ground-based telescopes can in principle make such observations when fitted with ground-layer adaptive optics (GLAO)[4–6], which removes the optical aberration caused by atmospheric turbulence up to an altitude of ~500 m (refs 7-10). A GLAO system that uses multiple laser guide stars[11–13] has been developed at the 6.5-m MMT telescope, in Arizona. In previous tests[13], the system improved the resolution of the telescope by 30–50%, limited by wavefront error in the optics, but that was insufficient to allow rapid determination of cluster membership. Here we report observations of the core of the globular cluster M3 made after commissioning a sensor to monitor and remove slowly varying aberration in the optics. In natural seeing of 0.7″, the point spread function at 2.2-μm wavelength was sharpened uniformly to 0.3″ over a field of at least 2′. The wide-field resolution was enhanced by a factor of two to three over previous work[13], with better uniformity, and extends to a wavelength of 1.2 μm. Entire stellar clusters may be examined in a single pointing, and cluster membership can be determined from two such observations separated by just one year[14–17].

The potential of GLAO to meet all these observational requirements has been predicted by analytic studies[8] and numerical simulations[18,19]. Preliminary results[13] from the optical system built at the MMT to implement GLAO also hinted at the ability of the technique to offer wide-field near-infrared image sharpening, but that work was limited by aberration in the optical train of the laser-guide-star wavefront sensor that was not seen by the science camera.

The MMT system projects five pulsed laser beams, each of power ~4 W and wavelength 532 nm, from a single telescope of 50-cm diameter positioned behind the MMT's secondary mirror. They are arranged in a regular pentagon spanning a field of 2′. A Shack–Hartmann wavefront sensor records the light returned to the telescope by Rayleigh backscattering of each laser pulse over a range from 20 to 29 km (ref. 12). The beacon light is maintained in sharp focus over this range by means of a mirror in the optical train that oscillates longitudinally at a frequency equal to the laser pulse rate[11]. The signals from the five beacons are sensed separately and then averaged to obtain the mean wavefront, representing our estimate of the ground-layer aberration. Because of unknown jitter in the outgoing laser beam paths, overall image motion in the MMT's focal plane is not measurable by the Shack–Hartmann sensor. Instead, a separate tilt sensor looking at a nearby natural star is used to recover that information. Both sensors run at 400 frames per second. A beam splitter ahead of the tilt sensor directs 10% of the light from the natural star to a third sensor of high spatial order. This sensor is read only once every 10–30 s; its output, calibrated against an unresolved source in the optical system, is used to determine and correct the aberrations that are not common to the optical paths of the wavefront sensor and the science camera. This use of the third sensor has proved critical in achieving the system's predicted performance.

The MMT's unique adaptive secondary mirror[20] is used to correct the aberrations measured by all three sensors. Because the mirror is large and conjugates to the low atmospheric layers to be corrected, it naturally provides correction over a wide field while eliminating the losses and added thermal emission of conventional adaptive optics[21]. Updates to the mirror actuators are synchronized with the fast sensor read-outs. The resulting image in the near infrared is recorded by an imaging camera, called PISCES, that is sensitive from 1.2 to 2.5 μm and has a 110″ field of view and a 0.1″ pixel scale[22].

Images of the globular cluster M3 were recorded in wavebands centred on 1.25 μm (J), 1.65 μm (H) and 2.15 μm (K). To illustrate, in Fig. 1 we present details of two observations of M3 taken in the K band. Each is a 60-s exposure comprising the sum of 60 individual 1-s images taken over a 4-min period. The first observation (Fig. 1a) was recorded with no adaptive optics correction but with the adaptive secondary mirror set to a fixed position that removed as far as possible the static wavefront aberration introduced by the telescope and instrument optics. In this case, the stellar images reflect the native seeing of 0.7″, which is slightly worse than the median at the MMT at this wavelength, 0.60″. The second observation shows the image quality obtained with GLAO: the average image width across the entire field is reduced to 0.30″. Figure 1b–e shows the results, with and without adaptive correction, in two 27″ × 27″ regions of the field, one centred on the tip–tilt star and the other centred near the edge of the camera's field. Each subfield is about the size of the isoplanatic patch for conventional adaptive optics correction at this wavelength. We note that the point spread function (PSF) is nearly identical in the two subfields. Furthermore, the peak intensity of the stellar images was improved over the full field by an average factor of 3.4, which for a detection at a given signal-to-noise ratio leads to an improvement of 2 mag in this very crowded region. Although the correction does not reach the diffraction limit, which at this wavelength is 0.07″, the image quality is essentially constant across the field of view; the standard deviation of the full-width at half-maximum (FWHM) is 0.009″.

We have examined the behaviour of the PSF from observations in the J, H and K bands of the open star cluster M34, which is less crowded than M3 and allows individual stellar images to be well isolated for this purpose. Properties of the PSF are summarized in

[1]Steward Observatory, The University of Arizona, Tucson, Arizona 85721, USA. [2]Caltech Optical Observatories, California Institute of Technology, Pasadena, California 91125, USA. [3]W. M. Keck Observatory, 65-1120 Mamalahoa Highway, Kamuela, Hawaii 96743, USA.

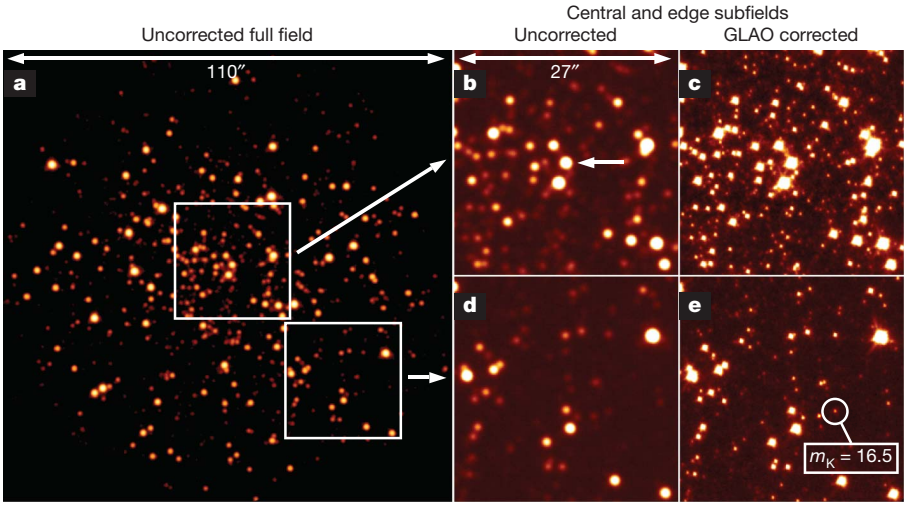

Figure 1 | The core of M3 imaged in the K band in two 60-s exposures in May 2009. a, The full 110″ field of our infrared camera in the native seeing limit of 0.7″, on a logarithmic intensity scale. **b**, **d**, Two smaller 27″ regions of the same image, indicated by the boxes in **a**, shown on a truncated linear scale in which bright stars appear saturated but which reaches the noise floor and brings out the faintest observable stars: one (**b**) is centred on the tip–tilt star, indicated by the arrow, and the other (**d**) is positioned to show the edge of the field. **c**, **e**, In a second 60-s exposure of the same two regions, taken with GLAO running at 400 Hz, and shown on the same linear scale as **b** and **d**, the stellar image width is reduced to 0.3″ and the PSF morphology is very similar across the whole field of view. For reference, we highlight a star in the corrected image with K-band magnitude $m_K = 16.5$, detected at a signal-to-noise ratio of 26. In the uncorrected image, stars must be 2 mag brighter to be seen at the same signal-to-noise ratio.

Table 1. In Fig. 2a, we show the FWHM of stellar images as a function of angular separation from the tilt star, measured from 60-s exposures recorded in the K band with and without GLAO correction. The mean uncorrected FWHM in this case was 0.61″, and this improved to 0.22″ with correction. We note that no trend in corrected image width across the field is apparent. The standard deviation is just 0.016″, attributable to the 0.015″ mean estimated uncertainty, arising largely from sky background noise, in the measurement of individual FWHM values. The reduction in FWHM represents an improvement in seeing from average to better than the fifth percentile for the site. Of particular importance to spectroscopy, which is improved with higher energy concentration, is that the encircled energy flux within a 0.2″ circular aperture increased substantially in all wavebands. So did the peak intensity, which in the case of the K band improved from 1.2% to 6.7% of the value of the diffraction limit. No statistically significant trend with field angle is distinguishable for any of these metrics. Furthermore, observed ellipticity in the PSFs seems to be randomly distributed in position angle, with magnitudes between 0.0 and 0.3 that are consistent in each case with a true value of zero. In short, we do not see any evidence for PSF variation across the field of view. Rather, GLAO correction was fully effective over at least 2′, suggesting that the improvement will be significant over substantially larger fields.

Radial stellar image profiles were computed in all three wavebands by averaging the images of the same 25 stars across the field that were used to characterize the GLAO performance in Fig. 2a. The positions of the stars in the field are plotted in Fig. 2b and the profiles are shown in Fig. 2c. The best image sharpening was as expected in the K band, but, remarkably, the system is still effective at correcting in the J band. The performance in the H and K bands is in line with the results predicted by numerical modelling: approximately 0.2″ ± 0.05″ for the K band[18,19] and 0.3″ ± 0.05″ for the H band[19], depending on assumed conditions. But the best performance expected at the shorter wavelength for the approximately median conditions actually observed in this experiment is around 0.4″. The result is arguably attributable to an unusually low and thin ground layer during this observation, or a high ratio of ground-layer to free-atmosphere turbulence, but performance in the J band that exceeds the modelling predictions has now been observed during several telescope runs under a variety of seeing conditions and at different times of year.

Table 1 | Properties of the compensated point spread function

Waveband	FWHM	Encircled energy enhancement*	Peak intensity enhancement
K (2.2 μm)	0.22″	3.8	5.5
H (1.65 μm)	0.29″	2.7	3.6
J (1.25 μm)	0.29″	2.3	3.0

* The factor by which the energy within a 0.2″ circular aperture is increased by GLAO.

Examination of the individual 1-s exposures of M3 shows that for the bright stars, relative astrometric accuracy is proportional to $1/\sqrt{t_{int}}$, where t_{int} is the total integration time, as expected from differential tilt jitter along the different lines of sight[23]. The standard deviation for the measured positions of stars of K-band magnitude $m_K = 16$ is 7.0 mas over the full field in the 1-s exposures, which reduces to 1.3 mas in co-additions of 30-s total exposure. Provided that care is taken to avoid systematic effects from optical distortion in the instrument and differential atmospheric refraction[3], the error will continue to scale as $1/\sqrt{t_{int}}$ and also as $1/\sqrt{B}$, where B is the brightness of the star. Extrapolating from the M3 observations, we find that the required accuracy of 0.2 mas for stars of $m_K = 18$ will be achieved in an integration time of 7,700 s.

The MMT's GLAO system is the first of its kind, designed as a prototype for more capable systems on larger telescopes. Nonetheless, performance, even at this early stage in the development of the technique, compares favourably with space-based instruments intended to address similar scientific goals. The Wide Field Camera 3 on the Hubble Space Telescope is the latest such instrument. It offers imaging and low-resolution slitless spectroscopy over a field of view of 135″ × 123″, sampled with rectangular 0.135″ × 0.121″ pixels, and wavelength coverage from 800 to 1,700 nm in its infrared channel. The field of view and spatial resolution are similar to those of the PISCES camera at the MMT with GLAO, and because the MMT has a collecting area 7.8-fold bigger than that of the Hubble Space Telescope, energy concentration in the core of the PSF is also similar. But the great versatility of GLAO lies in its broad applicability: it is not tied to any particular instrument.

Building on the work at the MMT, a similar system is now under construction for use with the Large Binocular Telescope, in Arizona[24], which also deploys adaptive secondary mirrors. Two instruments, collectively called LUCIFER[25], one on each half of the Large Binocular Telescope and each with a field of view of 4′, offer both imaging and multi-object spectroscopy in the J, H and K bands. Supplied with GLAO-corrected images, they will undertake rapid spectroscopic and astrometric surveys of large areas of the sky, with

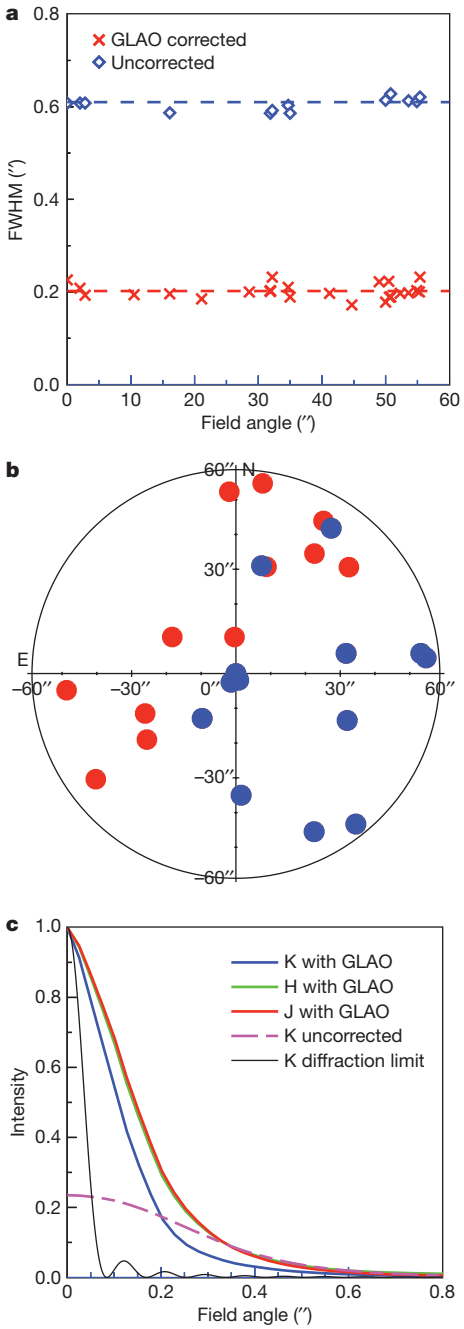

Figure 2 | Comparison of open-loop and closed-loop near-infrared image widths. **a**, In the K band, the corrected stellar images in M34 show no more significant variation in FWHM versus separation from the tip–tilt star (spectral type A1, $m_K = 10.0$) across the PISCES field than they do in the seeing limit. The horizontal dotted lines represent the average corrected FWHM (red; 0.22″) and uncorrected FWHM (blue; 0.61″, about median for the site). In both cases, the FWHM was measured for all stars detected with a signal-to-noise ratio greater than 20, which yielded sample sizes of 13 and 25 in the open- and closed-loop cases, respectively. **b**, The stars' placement in the field. Red points indicate stars measured in closed loop, and blue points indicate those measured in both open loop and closed loop. **c**, Radial profiles of the GLAO-corrected images, normalized to unit peak intensity, in the J, H and K wavebands have FWHMs of 0.29″, 0.29″ and 0.22″, respectively. The remarkable degree of similarity between the J and H profiles is, we believe, attributable to statistical fluctuations in the seeing. Also shown, for comparison, are the seeing-limited K-band image profile, normalized to the same total energy as the corrected K-band image, and the profile expected of a diffraction-limited source in the K band.

dozens of objects examined in a single exposure. GLAO effectively improves the site seeing by a factor of two to three over a wide field, thereby increasing the effective telescope aperture by a similar factor in regard to its sensitivity to unresolved sources. It therefore allows the study of many important topics, ranging from the formation and aggregation of galaxies in the early Universe and the origin of the Hubble sequence to determining the initial mass function of massive young star clusters.

Received 19 March; accepted 24 June 2010.

1. McCrady, N., Graham, J. R. & Vacca, W. D. Mass segregation and the initial mass function of super star cluster M82-F. *Astrophys. J.* **621,** 278–284 (2005).
2. Stolte, A., Brandner, W., Grebel, E. K., Lenzen, R. & Lagrange, A.-M. The Arches cluster: evidence for a truncated mass function? *Astrophys. J.* **628,** L113–L117 (2005).
3. Cameron, P. B., Britton, M. C. & Kulkarni, S. R. Precision astrometry with adaptive optics. *Astron. J.* **137,** 83–93 (2009).
4. Angel, J. R. P. & Lloyd-Hart, M. Atmospheric tomography with Rayleigh laser beacons for correction of wide fields and 30 m class telescopes. *Proc. SPIE* **4007,** 270–276 (2000).
5. Rigaut, F. in *Beyond Conventional Adaptive Optics* (eds Vernet, E., Ragazzoni, R., Esposito, S. & Hubin, N.) 11–16 (Proc. ESO 58, European Southern Observatory, 2002).
6. Lloyd-Hart, M. *et al.* Experimental results of ground-layer and tomographic wavefront reconstruction from multiple laser guide stars. *Opt. Exp.* **14,** 7541–7551 (2006).
7. Marchetti, E. *et al.* On-sky testing of the Multi-Conjugate Adaptive Optics Demonstrator. *Messenger* **129,** 8–13 (2007).
8. Tokovinin, A. Seeing improvement with ground-layer adaptive optics. *Publ. Astron. Soc. Pacif.* **116,** 941–951 (2004).
9. Martin, O. *et al.* Opto-mechanical commissioning of the GLAS Rayleigh laser guide star for the WHT. *Proc. SPIE* **7015,** 70154N (2008).
10. Tokovinin, A. *et al.* SAM: a facility GLAO instrument. *Proc. SPIE* **7015,** 70154C (2008).
11. Stalcup, T. *et al.* Field tests of wavefront sensing with multiple Rayleigh laser guide stars and dynamic refocus. *Proc. SPIE* **5490,** 1021–1032 (2004).
12. Lloyd-Hart, M. *et al.* First tests of wavefront sensing with a constellation of laser guide beacons. *Astrophys. J.* **634,** 679–686 (2005).
13. Baranec, C. *et al.* On-sky wide-field adaptive optics correction using multiple laser guide stars at the MMT. *Astrophys. J.* **693,** 1814–1820 (2009).
14. Reid, M. J. *et al.* Trigonometric parallaxes of massive star-forming regions. VI. Galactic structure, fundamental parameters, and noncircular motions. *Astrophys. J.* **700,** 137–148 (2009).
15. Stolte, A. *et al.* The proper motion of the Arches cluster with Keck laser-guide star adaptive optics. *Astrophys. J.* **675,** 1278–1292 (2008).
16. Hußmann, B., Stolte, A. & Brandner, W. in *Star Clusters: Basic Galactic Building Blocks throughout Time and Space* (eds de Grijs, R. & Lépine, J. R. D.) 422 (Proc. Int. Astron. Union 5 Symp. S266, International Astronomical Union, 2010).
17. Schödel, R., Merritt, D. & Eckart, A. The nuclear star cluster of the Milky Way: proper motions and mass. *Astron. Astrophys.* **502,** 91–111 (2009).
18. Andersen, D. *et al.* Performance modeling of a wide-field ground-layer adaptive optics system. *Publ. Astron. Soc. Pacif.* **118,** 1574–1590 (2006).
19. Le Louarn, M. & Hubin, N. Improving the seeing with wide-field adaptive optics in the near-infrared. *Mon. Not. R. Astron. Soc.* **365,** 1324–1332 (2006).
20. Wildi, F., Brusa, G., Lloyd-Hart, M., Close, L. & Riccardi, A. First light of the 6.5-m MMT adaptive optics system. *Proc. SPIE* **5169,** 17–25 (2003).
21. Lloyd-Hart, M. Thermal performance enhancement of adaptive optics by use of a deformable secondary mirror. *Publ. Astron. Soc. Pacif.* **112,** 264–272 (2000).
22. McCarthy, D., Ge, J., Hinz, J., Finn, R. & de Jong, R. PISCES: a wide field 1–2.5 micron camera for large aperture telescopes. *Publ. Astron. Soc. Pacif.* **113,** 353–361 (2001).
23. Sasiela, R. J. *Electromagnetic Wave Propagation in Turbulence: Evaluation and Application of Mellin Transforms* 2nd edn, 164–172 (Springer Ser. Wave Phenomena, Springer, 1994).
24. Rabien, S. *et al.* The laser guide star program for the LBT. *Proc. SPIE* **7015,** 701515 (2008).
25. Mandel, H. *et al.* LUCIFER: a NIR spectrograph and imager for the LBT. *Astron. Nachr.* **328,** 626–627 (2007).

Acknowledgements We thank the staff of the Steward Observatory Engineering and Technical Services division and the staff of the MMT Observatory for their support in the development and deployment of the MMT adaptive optics system. We are grateful to P. Strittmatter and R. Angel for reading the manuscript. The observations reported here were made at the MMT Observatory, a joint facility of The University of Arizona and the Smithsonian Institution. The work has been supported by the National Science Foundation.

Author Contributions M.H. wrote the paper. N.M.M., C.B., M.H. and E.B. carried out the data reduction. N.M.M. designed the adaptive optics reconstructor matrices. K.P. analysed the real-time system performance. T.S. designed and built the laser launch optics and wrote the system's operating software. D.M. and C.K. operated the infrared camera that recorded the cluster images at the telescope. All authors took part in the telescope runs during which the data presented here were acquired.

Author Information Reprints and permissions information is available at www.nature.com/reprints. The authors declare no competing financial interests. Readers are welcome to comment on the online version of this article at www.nature.com/nature. Correspondence and requests for materials should be addressed to M.H. (mhart@as.arizona.edu).